J|A|C|S
ARTICLES
Published on Web 11/20/2003

Assembly of an Electronically Switchable Rotaxane on the Surface of a Titanium Dioxide Nanoparticle

Brenda Long, Kirill Nikitin, and Donald Fitzmaurice*

Contribution from the Department of Chemistry, University College Dublin, Belfield, Dublin 4, Ireland

Received July 29, 2003; E-mail: donald.fitzmaurice@ucd.ie

Abstract: This paper describes the self-assembly of a heterosupramolecular system consisting of a tripodal [2]rotaxane adsorbed at the surface of a titanium dioxide nanoparticle. The tripodal [2]rotaxane consists of a dumbbell-shaped molecule, incorporating two electron-poor viologens, threading an electron-rich crown ether. The [2]rotaxane also incorporates a bulky tripodal linker group at one end and a bulky stopper group at the other end. The [2]rotaxane is adsorbed, via the tripodal linker group, at the surface of a titanium dioxide nanoparticle. The structure and function of the resulting hetero[2]rotaxane have been studied in detail by ^{1}H NMR spectroscopy and cyclic voltammetry. A key finding is that it is possible to electronically address and switch the above hetero[2]rotaxane.

Introduction

A goal shared by researchers in many fields is the bottom-up assembly of functional nanoscale architectures in solution and at technologically relevant substrates.[1] Expected benefits include greater control over material properties and innovative technologies that address unmet needs.[2] The self-assembly of molecular and nanoscale condensed phase components in solution and their self-organization at a suitably patterned substrate is a possible approach.[3]

In considering what molecular and condensed phase components might make such an approach possible;[4−6] one is attracted to functional supermolecules[7] and to the rapidly growing number of nanoparticles whose properties can be tuned by controlling their size and surface composition.[8] It is in this context that we have sought to synthesize molecular components that are adsorbed at the surface of a nanoparticle; orientated normal to the surface of the nanoparticle; displaced from the nanoparticle in order to avoid unwanted surface effects; and finally, sufficiently bulky to preclude unwanted lateral interactions.

A class of functional supermolecule that has attracted a great deal of attention are the rotaxanes.[9] A class of nanoparticle that has attracted a great deal of attention are metal oxides.[10]

Accordingly, we have designed and synthesized the tripodal [2]rotaxane shown in Scheme 1. The phosphonate moieties of the linker group bind the viologen to the surface of a titanium dioxide nanoparticle. The rigid tripodal arrangement of these phosphonate moieties orients the viologens normal to and displaces them from the surface of the nanoparticle. The inherent bulkiness of the tripodal linker reduces the possibility of pimerization of the reduced viologens.[11] As a consequence, the crown ether is free to shuttle between the viologens. The structure and function of the resulting hetero[2]rotaxane have been studied in detail by ^{1}H NMR spectroscopy and cyclic voltammetry. A key finding is that it is possible to electronically address and switch the above hetero[2]rotaxane.

It should be noted that Galoppini and Meyer and their respective co-workers have recently described the synthesis of tripodal linkers used to adsorb sensitizer molecules at the surface of the constituent titanium dioxide nanoparticles of a nanostructured film forming the anode of a regenerative photoelectrochemical cell.[12]

It should also be noted that Fitzmaurice and co-workers have recently described the synthesis of a tripodal viologen that is adsorbed at the surface of a titanium dioxide nanoparticle and is capable of threading a crown ether to from a hetero[2]-pseudorotaxane.[13,14] The syntheses of the tripodal viologen and related molecular components employed in this study are described in the Supporting Information.[15]

Finally, the findings reported here are also significant in the context of the related findings recently reported by Balzani and

(1) Philp, D.; Stoddart, J. F. *Angew. Chem., Int. Ed. Engl.* **1996**, *35*, 1154.
(2) Bows, W. *Investors Chronicle* **2002**, *139*, 30.
(3) Whitesides, G. M.; Mathias, J. P.; Seto, C. T. *Science* **1991**, *254*, 1212.
(4) Service, R. F. *Science* **1997**, *277*, 1036.
(5) Mann, S.; Shenton, W.; Li. M.; Connolly, S.; Fitzmaurice, D. *Adv. Mater.* **2000**, *12*, 147.
(6) Niemeyer, C. *Angew. Chem., Int. Ed.* **2001**, *40*, 4128.
(7) Lehn, J.-M. *Supramolecular Chemistry, Concepts and Perspectives*; VCH: Weinheim, 1995.
(8) Alivisatos, A. P. *Science* **1996**, *271*, 933.
(9) Stoddart and co-workers. *J. Am. Chem. Soc.* **1996**, *118*, 4931.
(10) Hagfeldt, A.; Gratzel, M. *Chem. Rev.* **1995**, *95*, 49.
(11) Felderhoff, M.; Heinen, S.; Molisho, N.; Webersinn, S.; Walder, L. *Helv. Chim. Acta* **2000**, *83*, 181.
(12) (a) Galoppini, E.; Guo, W. *J. Am. Chem. Soc.* **2001**, *123*, 4342. (b) Galoppini, E.; Guo, W.; Zhang, W.; Hoetz, P. G.; Qu, P.; Meyer, G. J. *J. Am. Chem. Soc.* **2002**, *124*, 7801.
(13) (a) Nikitin, K.; Long, B.; Fitzmaurice, D. *J. Chem. Soc., Chem. Commun.* **2003**, 282. (b) Long, B.; Nikitin, K.; Fitzmaurice, D. *J. Am. Chem. Soc.* **2003**, *125*, 5152.
(14) (a) Fitzmaurice, D.; Rao, S. N.; Preece, J. A.; Stoddart, J. F.; Wenger, S.; Zaccheroni, N. *Angew. Chem., Int. Ed.* **1999**, *38*, 1147. (b) Ryan, D.; Rao, S. N.; Rensmo, H.; Fitzmaurice, D.; Preece, J. A.; Wenger, S.; Stoddart, J. F.; Zaccheroni, N. *J. Am. Chem. Soc.* **2000**, *122*, 6252.
(15) See the Supporting Information.

10.1021/ja037592g CCC: $25.00

Scheme 1. Electronically Addressable and Switchable Hetero[2]rotaxane

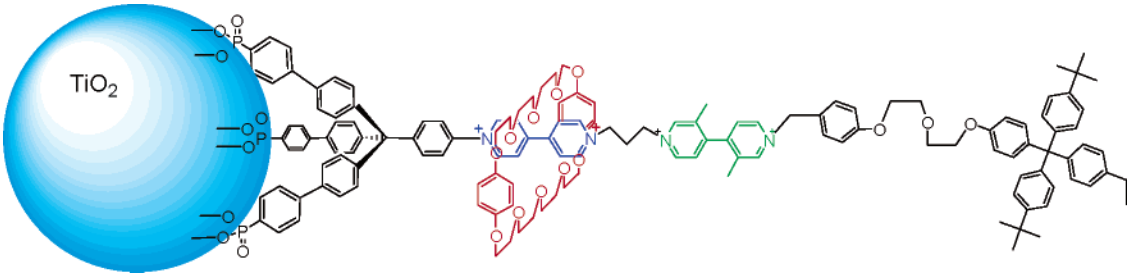

Table 1. Proton Nuclear Magnetic Resonance Data

	V_1				V_2						
	2	2′	3	3′	2	2′	2	2′	3	3′	C
TiO_2•**1R**					8.85	8.76		8.71	7.80	7.68	6.44
TiO_2•**1**					8.88	8.78			7.95	7.89	6.24
TiO_2•**2**					8.86	8.76		8.58	7.96	7.88	
TiO_2•**3R**											
TiO_2•**3**											6.16
TiO_2•**4**											
5											6.77

Stoddart and co-workers[16] and more recently by Heath and Stoddart and co-workers.[17]

Results and Discussion

Design and Synthesis of Tripodal [2]Rotaxanes. The tripodal [2]rotaxanes (**1** and **3**) and corresponding tripodal axles (**2** and **4**, respectively), along with the crown ether **5** and nanoparticle stabilizer **6** employed in the present study, are shown in Scheme 2.

The design and synthesis of tripodal [2]pseudorotaxanes that are capable of being adsorbed normal to and displaced from the surface of a titanium dioxide nanoparticle have been described in detail elsewhere.[13] These design principles and synthetic strategies have been extended to the preparation of tripodal [2]rotaxanes (and the corresponding tripodal axle components), which are also capable of being adsorbed normal to and displaced from the surface of a titanium dioxide nanoparticle.[15]

In the case of the tripodal [2]rotaxane **1**; the ester analogue of the tripodal bis-viologen, the crown **5**, and the bulky stopper were all synthesized as described in the Supporting Information.[15] These subcomponents were subsequently self-assembled under ambient conditions to form the ester analogue of the tripodal [2]rotaxane **1** in high yield. The ester analogues of the tripodal [2]rotaxane **3** and the corresponding tripodal axle components **2** and **4**, respectively, were prepared using a similar approach.[15]

The target tripodal [2]rotaxanes **1** or **3** and the corresponding axle components (**2** and **4**, respectively) were obtained by hydrolysis of the phosphonic ester groups at the end of the tripod legs to yield the corresponding phosphonic acid groups.

There are a number of known methods that can be used to hydrolyze a phosphonic ester to the corresponding phosphonic acid. However, the usefulness of these known methods is limited in the cases of compounds **1** to **4**. Methods involving base hydrolysis may not be used, as the viologen moieties are not stable under these conditions. Methods based on acidic hydrolysis at elevated temperatures are not applicable, as the ethoxyethylene moieties are not stable under these conditions. For these reasons, a novel method has been developed for this step that employs trimethylsilyl bromide in 1,4-dioxane at ambient temperature. Using this method, the ester groups can be selectively hydrolyzed.[13b] The method for separating compounds **1** to **4** from unwanted side products, formed mainly from 1,4-dioxane, exploits their exceptionally high solubility in concentrated aqueous HCl.

Adsorption of Tripodal [2]Rotaxanes at the Surface of a Nanoparticle. A charge stabilized dispersion of titanium dioxide nanoparticles (6 nm diameter) was prepared by hydrolysis of titanium orthotetraisopropoxide in water at pH 2.[18] The tripodal [2]rotaxanes **1** and **3**, and the corresponding tripodal axle components (**2** and **4**, respectively), readily chelate Ti^{4+} states at the surface of the above nanoparticles and are adsorbed. The number of Ti^{4+} sites on the surface of each nanoparticle was estimated, based on literature values for the number of such states (2×10^{14} cm^{-2}), to be 226.[19] An average of 12 tripodal [2]rotaxanes, or the corresponding tripodal axles, were adsorbed at the surface of each titanium dioxide nanoparticle. Molecular modeling reveals that the footprint of a tripodal linker is 144 $Å^2$ and that the area occupied on the surface of a nanoparticle by 12 adsorbed tripodal viologens is 1728 $Å^2$ corresponding to 15% of the available surface area. The partially deuterated stabilizer **6** was adsorbed at the remaining Ti^{4+} sites on the surface of each nanoparticle.[13] These nanoparticles were precipitated from the above aqueous dispersion by addition of ammonium hexafluorophosphate, washed with dry methanol, and redispersed in acetonitrile to form a stable optically transparent dispersion.

Structural Characterization of Tripodal Hetero[2]rotaxanes by Proton NMR. The ^1H NMR spectra of TiO_2•**1** and TiO_2•**2** were recorded with a view to establishing that the tripodal [2]rotaxane **1** and the corresponding axle component **2** are adsorbed normal to and displaced from the surface of the TiO_2 nanoparticle in TiO_2•**1** and TiO_2•**2**, respectively. See expanded aromatic region in Figure 1 and also Scheme 3 and Table 1.

It is concluded, based on the finding that the resonances assigned to protons of the tripodal linker **L** and the viologen $\mathbf{V}_1$ adjacent to **L** in TiO_2•**1** are suppressed, that **1** is adsorbed at the surface of the titanium dioxide nanoparticle in TiO_2•**1**. Specifically, it is found that the following resonances are

(16) Ashton, P. R.; Ballardini, R.; Balzani, V.; Credi, A.; Ruprecht-Dress, K.; Ishow, E.; Kleverlaan, C.; Kocian, O.; Preece, J.; Spencer, N.; Stoddart, J. F.; Venturi, M.; Wenger, S. *Chem.—Eur. J.* **2000**, *6*, 3558.
(17) (a) Collier, C. P.; Wong, E. W.; Belohradsky, M.; Raymo, F. M.; Stoddart, J. F.; Kuekes, P. J.; Williams, R. S.; Heath, J. R. *Science* **1999**, *285*, 391. (b) Collier, C. P.; Mattersteig, G.; Wong, E. W.; Luo, Y.; Beverly, K.; Sampaio, J.; Raymo, F. M.; Stoddart, J. F.; Heath, J. R. *Science* **2000**, *289*, 1172.
(18) O'Reagen, B.; Graetzel, M. *Nature* **1991**, *353*, 737.
(19) Finklea, H. O. *Semiconductor Electrodes*; Elsevier: 1988.

Scheme 2. Molecular Components

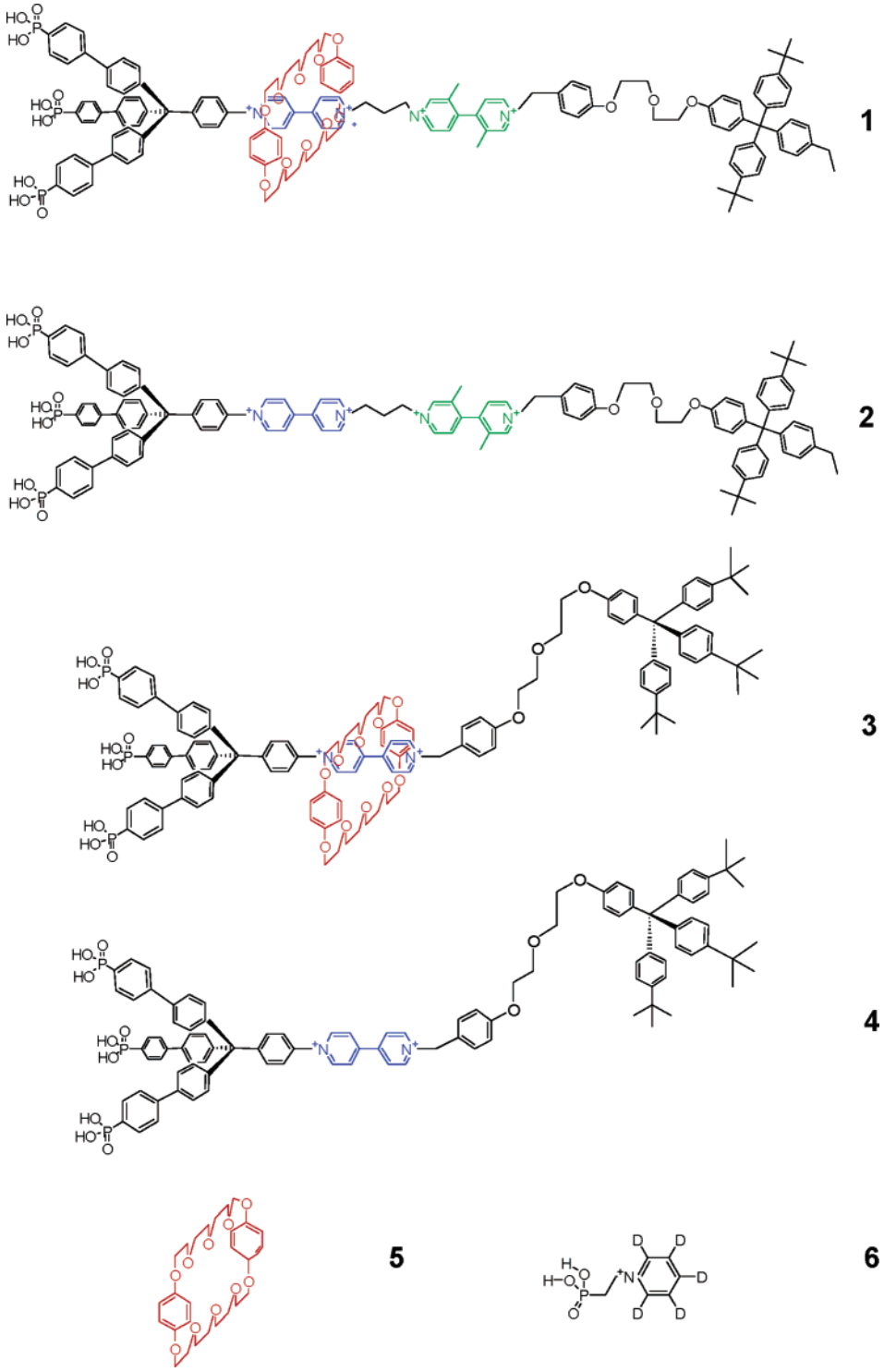

suppressed: δ 9.1 (2-position of $\mathbf{V_1}$), 8.8 (2′-position of $\mathbf{V_1}$), 8.0 (3-position of $\mathbf{V_1}$), 7.9 (3′-position of $\mathbf{V_1}$), 7.7 (phosphorylated *p*-phenylenes of **L**), 7.6 (phosphorylated *p*-phenylenes of **L** and *p*-phenylene link to $\mathbf{V_1}$), 7.5 (*p*-phenylene of **L**), 7.3 (*p*-phenylene of **L**), 4.8 (methylene group adjacent to $\mathbf{V_1}$ of trimethylene bridge linking viologens), and 2.9 (central methylene group of trimethylene bridge linking viologens).

It is concluded, based on the finding that the resonances assigned to protons of the bulky stopper **S** and the viologen $\mathbf{V_2}$ adjacent to **S** in TiO_2•**1** are broadened, that **L** and $\mathbf{V_1}$ of **1** are orientated normal to and displaced from the surface of the nanoparticle and that $\mathbf{V_2}$ and **S** of **1** are free to undergo restricted rotational motion.

Specifically, it is found that the following proton resonances are broadened: δ 8.9 and 8.8 (2- and 2′-positions of $\mathbf{V_2}$), 7.8 and 7.7 (3-position of $\mathbf{V_2}$), 7.5 (3-position of *N*-benzyl), 7.3 (phenylenes of **S**), 7.2−7.0 (2-position of *N*-benzyl and phenylenes of **S**), 6.8 (2-position of the alkoxyphenylene group attached to the ether link), 6.2 (*p*-hydroxyphenylene of the crown **C**), 5.7 (methylene of *N*-benzyl), 4.8 (methylene group adjacent

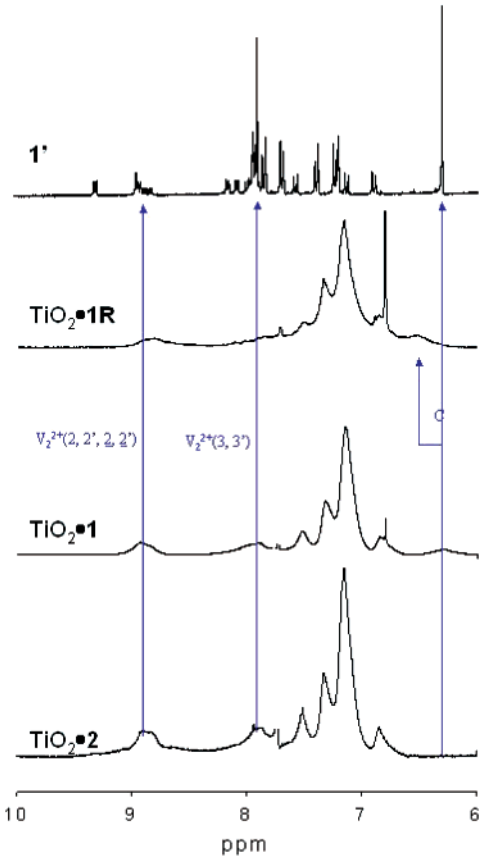

Figure 1. ^{1}H NMR spectra of **1′** (1.4×10^{-3} mol dm^{-3} molecules), TiO_2•**1** (1.2×10^{-4} mol dm^{-3} particles and 1.4×10^{-3} mol dm^{-3} molecules), and TiO_2•**2** (1.2×10^{-4} mol dm^{-3} particles and 1.4×10^{-3} mol dm^{-3} molecules) in acetonitrile-d_3 at 30° C. ^{1}H NMR spectra of TiO_2•**1R** (1.2×10^{-4} mol dm^{-3} particles and 1.4×10^{-3} mol dm^{-3} molecules) in acetonitrile-d_3 at 30 °C was recorded following degassing by bubbling with nitrogen and reduction addition of zinc metal in the presence of chromium chloride.

Scheme 3. Notation for NMR Assignments

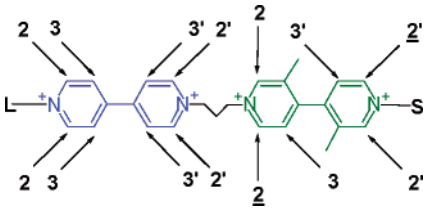

to $\mathbf{V_2}$ of trimethylene bridge linking viologens), 4.0 (ether link positions adjacent to aryloxy groups), 3.8 (rest of ether link positions and methylenes in **C**), 3.6−3.5 (methylene protons of **C**), 2.2 (methyl groups of $\mathbf{V_2}$), and 1.2 (*tert*-butyl groups of **S**).

It is concluded, based on the finding that the resonances assigned to protons of tripodal linker **L** and the viologen $\mathbf{V_1}$ of TiO_2•**2** are suppressed, that **2** is adsorbed at the surface of the titanium dioxide nanoparticle in TiO_2•**2**. Specifically, it is found that the following resonances are suppressed: δ 9.0 (2-position of $\mathbf{V_1}$), 8.9 (2′-position of $\mathbf{V_1}$), 8.4 (3-position of $\mathbf{V_1}$), 8.3 (3′-position of $\mathbf{V_1}$), 7.7 (phosphorylated *p*-phenylenes of **L**), 7.6 (phosphorylated *p*-phenylenes of **L** and *p*-phenylene link to $\mathbf{V_1}$), 7.4 (*p*-phenylene of **L**), 7.3 (*p*-phenylene of **L**), 4.7 (methylene group adjacent to $\mathbf{V_1}$ of trimethylene bridge linking viologens), and 2.9 (central methylene group of trimethylene bridge linking viologens).

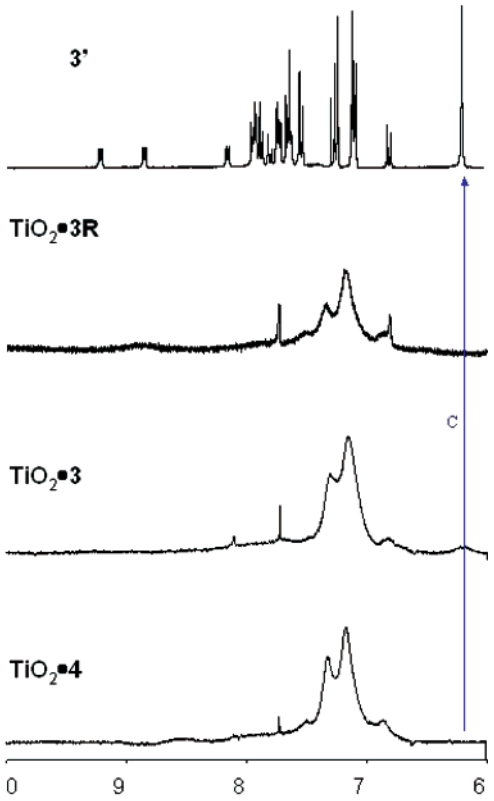

Figure 2. ^{1}H NMR spectra of **3′** (1.4×10^{-3} mol dm^{-3} molecules) in chloroform-*d* and methanol-d_4 (20% by vol) at 30 °C and of TiO_2•**4**, TiO_2•**3** (1.2×10^{-4} mol dm^{-3} particles and 1.4×10^{-3} mol dm^{-3} molecules), and TiO_2•**4** (1.2×10^{-4} mol dm^{-3} particles and 1.4×10^{-3} mol dm^{-3} molecules) in acetonitrile-d_3 at 30 °C. ^{1}H NMR spectra of TiO_2•**3R** (1.2×10^{-4} mol dm^{-3} particles and 1.4×10^{-3} mol dm^{-3} molecules) in acetonitrile-d_3 at 30 °C was recorded following degassing by bubbling with nitrogen and reduction addition of zinc metal in the presence of chromium chloride.

It is concluded, based on the finding that the resonances assigned to protons of the bulky stropper **S** and the viologen $\mathbf{V_2}$ adjacent to the bulky stopper in TiO_2•**2** are broadened, that **L** and $\mathbf{V_1}$ of **2** are orientated normal to and displaced from the surface of the nanoparticle and that $\mathbf{V_2}$ and **S** of **2** are free to undergo restricted rotational motion. Specifically, it is found that the following resonances are broadened: δ 8.9, 8.8, and 8.6 (the 2- and 2′-positions of $\mathbf{V_2}$); 7.9 and 7.8 (the 3-positions of $\mathbf{V_2}$); 7.5 (the 3-position of *N*-benzyl); δ 7.3 (phenylenes of **S**); 7.2−7.0 (2-position of *N*-benzyl and phenylenes of **S**); 6.8 (the 2-position of the alkoxyphenylene group of **S**); 5.7 (methylene of *N*-benzyl); 4.8 (methylene group adjacent to $\mathbf{V_2}$ of trimethylene bridge linking viologens); 4.1 (ether link positions adjacent to aryloxy groups), 3.8 (rest of ether link positions); 2.2 (methyl groups of $\mathbf{V_2}$); and 1.2 (*tert*-butyl groups of **S**).

The above findings allow us conclude that both **1** and the corresponding axle component **2** are adsorbed normal to but displaced from the surface of the TiO_2 nanoparticle in TiO_2•**1** and TiO_2•**2**, respectively. These findings are consistent with other recently reported findings.[12−14]

The ^{1}H NMR spectra of TiO_2•**3** and TiO_2•**4** were recorded with a view to establishing that the tripodal [2]rotaxane **3** and the corresponding axle component **2** were adsorbed normal to and displaced from the surface of the TiO_2 nanoparticle in TiO_2•**3** and TiO_2•**4**, respectively. See expanded aromatic region in Figure 2 and also Scheme 3 and Table 1.

It is concluded, based on the finding that the resonances assigned to protons of tripodal linker **L** and the viologen $\mathbf{V_1}$ of TiO_2•**3** are suppressed, that **3** is adsorbed at the surface of the titanium dioxide nanoparticle in TiO_2•**3**. Specifically, it is found that the following resonances are suppressed: δ 9.2 (2-position of $\mathbf{V_1}$), 8.8 (2′-position of $\mathbf{V_1}$), 8.2 (3-position of $\mathbf{V_1}$), 7.9 (3′-position of $\mathbf{V_1}$), 7.8 (phosphorylated *p*-phenylenes of **L**), 7.7 (phosphorylated *p*-phenylenes of **L** and *p*-phenylene link to $\mathbf{V_1}$), 7.6 (*p*-phenylene of **L**), 7.5 (the 3-position of *N*-benzyl), 7.5 (*p*-phenylene of **L**), and 5.9 (*N*-methylene).

It is concluded, based on the finding that the resonances assigned to protons of the bulky stopper **S** in TiO_2•**3** are broadened, that **3** is orientated normal to and displaced from the surface of the nanoparticle and free to undergo restricted rotational motion. Specifically, it is found that the following resonances are broadened: δ 7.3 (phenylenes of **S**), 7.2−7.0 (phenylenes of **S**), 6.8 (the 2-position of the alkoxyphenylene group of **S**), 6.2 (p-hyroxy-phenylene of **C**), 4.1 (ether link positions adjacent to aryloxy groups), 3.8 (rest of ether link positions and methylenes of **C**), 3.6−3.5 (methylene of **C**), and 1.2 (*tert*-butyl groups of **S**).

It is concluded, based on the finding that the resonances assigned to protons of tripodal linker **L** and the viologen $\mathbf{V_1}$ of TiO_2•**4** are suppressed, that **4** is adsorbed at the surface of the titanium dioxide nanoparticle in TiO_2•**4**. Specifically, it is found that the following resonances are suppressed: δ 9.0 (2-position of $\mathbf{V_1}$), 8.9 (2′-position of $\mathbf{V_1}$), 8.5 (3-position of $\mathbf{V_1}$), 8.4 (3′-position of $\mathbf{V_1}$), 7.8 (phosphorylated *p*-phenylenes of **L**), 7.7 (phosphorylated *p*-phenylenes of **L** and *p*-phenylene link to $\mathbf{V_1}$), 7.6 (*p*-phenylene of **L**), 7.5 (the 3-position of *N*-benzyl), 7.5 (*p*-phenylene of **L**), and 5.7 (*N*-methylene).

It is concluded, based on the finding that the resonances assigned to protons of the stopper group **S** in TiO_2•**4** are broadened, that **4** is orientated normal to and displaced from the surface of the nanoparticle and free to undergo restricted rotational motion. Specifically, it is found that the following resonances are broadened: δ 7.3 (phenylenes of **S**), 7.2−7.0 (phenylenes of **S**), 6.8 (the 2-position of the alkoxyphenylene group of **S**), 4.1 (ether link positions adjacent to aryloxy groups), 3.8 (rest of ether link positions), and 1.2 (*tert*-butyl groups of **S**).

The above findings allow us conclude that both **3** and the corresponding axle component **4** are adsorbed normal to but displaced from the surface of the TiO_2 nanoparticle in TiO_2•**3** and TiO_2•**4**, respectively. These findings are consistent with other recently reported findings.[12−14]

Dynamic Characterization of Tripodal Hetero[2]rotaxanes by Proton NMR. Shown in Figure 1 are the ^{1}H NMR spectra of **1′** in solution, the ester analogue of **1**, TiO_2•**1**, and TiO_2•**2**. Also shown is the spectrum of TiO_2•**1** following degassing by bubbling with nitrogen and reduction by addition of zinc metal in the presence of chromium chloride,[20,21] denoted TiO_2•**1R**. Given in Table 1, where resolved, are the chemical shifts of the aromatic proton resonances of $\mathbf{V_1}$ and $\mathbf{V_2}$ and of **C**.

In the discussion that follows, it is stated that **C** is localized at either $\mathbf{V_1}$ or $\mathbf{V_2}$. Such statements are intended to identify the thermodynamically favored translational isomer and the most probable location of **C**. They are not intended to suggest that C is stationed at $\mathbf{V_1}$ or $\mathbf{V_2}$.

Based on the finding that the resonance assigned to the aromatic protons of **C** in TiO_2•**1** is significantly upfield of the resonance for the same protons of **5** in solution, it is concluded that **C** in TiO_2•**1** is localized at $\mathbf{V_1}$ or $\mathbf{V_2}$. Specifically, it is found that the broadened resonance assigned to the aromatic protons of **C** is at δ 6.2 for TiO_2•**1**, while it is at δ 6.8 for **5** in solution. Based on the finding that the resonances assigned to the aromatic protons of the viologen $\mathbf{V_2}$ in TiO_2•**1** have similar chemical shifts in TiO_2•**2**, it is concluded that that **C** is localized at $\mathbf{V_1}$. Specifically, it is found that the broadened resonances assigned to the 2 and 2′ protons of $\mathbf{V_2}$ are observed at δ 8.9, δ 8.8, and δ 8.6 in both TiO_2•**1** and TiO_2•**2**. It is also found that that the broadened resonances assigned to the 3 and 3′ protons of $\mathbf{V_2}$ are observed at δ 8.0 and δ 7.9 in TiO_2•**1** and TiO_2•**2**. It should be noted that our conclusion **C** is localized at $\mathbf{V_1}$ in TiO_2•**1** is consistent with previously report findings[13] and with the fact that the affinity of **C** for $\mathbf{V_1}$ is an order of magnitude greater than for $\mathbf{V_2}$.[16]

Having established that **C** is initially localized at $\mathbf{V_1}$ in TiO_2•**1**, our interest turns to what happens when the viologen $\mathbf{V_1}$ is selectively chemically reduced to form TiO_2•**1R**. It might have been expected, based on previously reported findings,[16] that **C** would localize at $\mathbf{V_2}$, specifically, that the affinity of **C** for $\mathbf{V_2}$ would be greater than for the radical cation of $\mathbf{V_1}$.

Based on the finding that the resonance assigned to the aromatic protons of **C** in TiO_2•**1R** is significantly upfield of the same resonance of **5** in solution and significantly downfield of the same resonance in TiO_2•**1**, it is concluded that **C** in TiO_2•**1** is either localized at $\mathbf{V_2}$ or, as a result of $\mathbf{V_1}$ having been reduced, is interacting less strongly with the radical cation of $\mathbf{V_1}$. Specifically, it is found that the broadened resonance assigned to the aromatic protons of **C** is at δ 6.4 for TiO_2•**1R**, while it is at δ 6.2 for **C** in TiO_2•**1** and at δ 6.8 for **5** in solution.

Based on the finding that the resonances assigned to the 2 and 2′ and the 3 and 3′ protons of the viologen $\mathbf{V_2}$ in TiO_2•**1R** are not and are, respectively, shifted upfield with respect to the corresponding resonances in TiO_2•**1** and TiO_2•**2**, it is concluded that **C** in TiO_2•**1R** is interacting with $\mathbf{V_2}$. Specifically, it is found that the broadened resonances assigned to the 2 and 2′ protons of $\mathbf{V_2}$ are observed at δ 8.9, δ 8.8, and δ 8.6 in TiO_2•**1R**, TiO_2•**1**, and TiO_2•**2**. It is also found that that the broadened resonances assigned to the 3 and 3′ protons of $\mathbf{V_2}$ are observed at δ 7.8 and δ 7.7 in TiO_2•**1R** and at δ 8.0 and δ 7.9 in TiO_2•**1** and TiO_2•**2**.

These findings permit the conclusion that **C** in TiO_2•**1R** is interacting to a greater extent with $\mathbf{V_2}$, following reduction of $\mathbf{V_1}$. These findings, however, do not permit the conclusion that **C** is localized on $\mathbf{V_2}$ and not interacting with $\mathbf{V_1}$. In support of this view, and as discussed in detail below, a dynamic characterization of this system by cyclic voltammetry suggests that **C** still interacts with the radical cation of $\mathbf{V_1}$ in TiO_2•**1R**. It should be noted that this finding is not unexpected for the following reason: While the association constant for formation of a complex between **C** and $\mathbf{V_2}$ is an order of magnitude smaller than the association constant for formation of a complex between

(20) Evans, A. G.; Evans, J. C.; Baker, M. W. *J. Chem. Soc., Perkin Trans. 2* **1977**, 1781.
(21) Anelli, P. L.; Ashton, P. R.; Ballardini, R.; Balzani, V.; Delgado, M.; Gandolfi, M. T.; Goodnow, T. T.; Kaifer, A. E.; Philp, D.; Pietraszkiewicz, M.; Prodi, L.; Reddington, M. V.; Slavin, A. M. Z.; Spencer, N.; Stoddart, J. F.; Vincenti, C.; Williams, D. J. *J. Am. Chem. Soc*. **1992**, *114*, 193−218.

Table 2. Cyclic Voltammetry Data

	$V_1^{2+} \rightarrow V_1^{+\bullet}$	$V_1^{+\bullet} \rightarrow V_1^{\bullet\bullet}$	$V_2^{2+} \rightarrow V_2^{+\bullet}$	$V_2^{+\bullet} \rightarrow V_2^{\bullet\bullet}$	$V_2^{\bullet\bullet} \rightarrow V_2^{+\bullet}$	$V_2^{+\bullet} \rightarrow V_2^{2+}$	$V_1^{\bullet\bullet} \rightarrow V_1^{+\bullet}$	$V_1^{+\bullet} \rightarrow V_1^{2+}$
TiO_2•**1**	−0.756	−1.057	−1.182	−1.469	−1.309	−1.060	−0.947	−0.647
TiO_2•**2**	−0.646	−0.975	−1.145	−1.468	−1.355	−1.064	−0.975	−0.600
Δ	−0.110	−0.082	−0.037	−0.001	+0.044	+0.004	+0.028	−0.047
TiO_2•**3**	−0.699	−1.112					−1.065	−0.666
TiO_2•**4**	−0.614	−1.012					−0.963	−0.579
Δ	−0.085	−0.100					−0.102	−0.087

C, it may be comparable to that for the formation of a complex between **C** and the radical cation of $\mathbf{V_1}$ and **C**.[16]

Further insights are gained by undertaking a similar analysis of the hetero[2]rotaxane TiO_2•**3** and the corresponding axle component TiO_2•**4**, both incorporating a single viologen $\mathbf{V_1}$.

Shown in Figure 2 are the ^{1}H NMR spectra of **3′** in solution, the ester analogue of **3**, TiO_2•**3**, and TiO_2•**4**. Also shown is the spectrum of TiO_2•**3** following degassing by bubbling with nitrogen and reduction by addition of zinc metal in the presence of chromium chloride, denoted TiO_2•**3R**. Given in Table 1, where resolved, are the chemical shifts of the aromatic proton resonances of $\mathbf{V_1}$ and the aromatic proton resonances of **C**.

Based on the finding that the resonance assigned to the aromatic protons of **C** in TiO_2•**3** is significantly upfield of the same resonance of **5** in solution, it is concluded that **C** in TiO_2•**3** is localized at $\mathbf{V_1}$. Specifically, it is found that the broadened resonance assigned to the aromatic protons of **C** is at δ 6.2 for TiO_2•**3**, while it is at δ 6.8 for **5** in solution. As discussed above, the resonances assigned to the aromatic protons of the viologen $\mathbf{V_1}$ are not observed due to its proximity to the surface of the TiO_2 nanoparticle.

Having established that **C** is localized at $\mathbf{V_1}$ in TiO_2•**3**, our interest again turns to what happens when the viologen $\mathbf{V_1}$ is selectively chemically reduced to form TiO_2•**3R**. It might have been expected, based on previous reports,[16] that **C** would no longer be localized at $\mathbf{V_1}$. In practice, it is found that the resonance assigned to the aromatic protons of **C** is no longer observed.[20,21] On this basis, it is concluded that **C** remains associated with $\mathbf{V_1}$ following its one-electron reduction. It should be noted that this does not preclude the possibility that **C** is more loosely associated with the radical cation of $\mathbf{V_1}$. It should also be noted that these findings are consistent with those recently reported by us for a related hetero[2]pseudorotaxane[13] and with those reported below for the electrochemical characterization of TiO_2•**3**.

Dynamic Characterization of Tripodal Hetero[2]rotaxanes by Cyclic Voltammetry. Shown in Figure 3 are the cyclic voltammograms (CVs) of the tripodal hetero[2]rotaxane TiO_2•**1** and the corresponding axle component adsorbed at the surface of a TiO_2 nanoparticle TiO_2•**2**. The first and second peak reduction and peak reoxidation potentials of $\mathbf{V_1}$ and $\mathbf{V_2}$ are given in Table 2.

It is found that the first and second reduction potentials of $\mathbf{V_1}$ are shifted to more negative values by 110 mV and 82 mV, respectively, due to the presence of **C** in TiO_2•**1**. It is also found that the first and second reduction potentials of $\mathbf{V_2}$ are shifted to more negative values by 37 mV and 1 mV, respectively.

On this basis, it is concluded that initially **C** interacts with $\mathbf{V_1}$ in TiO_2•**1**. Accordingly, $\mathbf{V_1}$ undergoes a first one-electron reduction to form the corresponding radical cation at more negative potentials than in the corresponding axle TiO_2•**2**. On this basis, it is also concluded that **C** continues to interact with

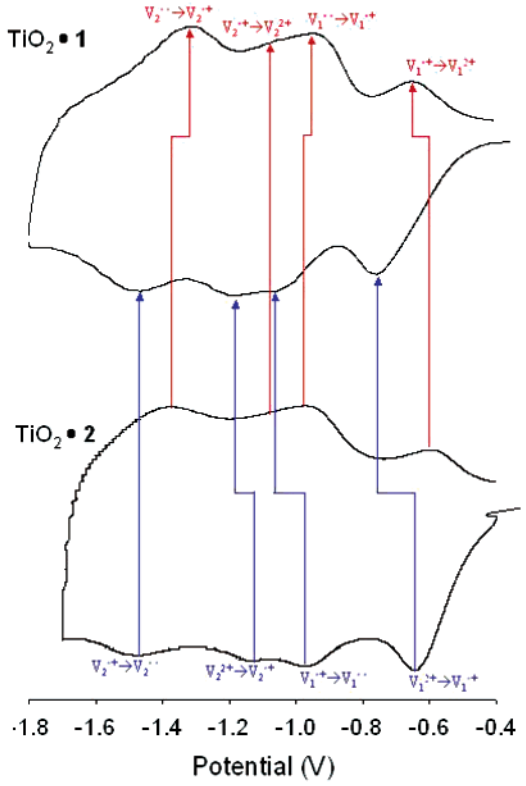

Figure 3. Cyclic voltammograms of nanostructured TiO_2 film (geometric area of 0.8 cm^2, surface roughness of 1000) modified by adsorption of **1** (5×10^{16} molecules) and **2** (5×10^{16} molecules) recorded in acetonitrile containing added TBAP (0.1 mol dm^{-3}) at 25 °C.

the singly reduced viologen $\mathbf{V_1}$. This accounts for the fact that the radical cation of $\mathbf{V_1}$ undergoes a second one-electron reduction at more negative potentials than the same viologen in the corresponding axle TiO_2•**2**.

This finding suggests that the affinity of **C** for $\mathbf{V_2}$ is less than or similar to the affinity of **C** for the radical cation of $\mathbf{V_1}$ and that **C** continues to interact with $\mathbf{V_1}$ even after this viologen has been reduced. This is perhaps not surprising when one takes into account that the affinity of **C** for $\mathbf{V_2}$ is 10 times lower than its affinity for $\mathbf{V_1}$.[16] It was nevertheless expected that, following the two successive one-electron reductions of $\mathbf{V_1}$ in TiO_2•**1**, that **C** would favor interaction with the doubly positively charged viologen $\mathbf{V_2}$.

Consistent with this expectation is the finding that the first reduction potential of $\mathbf{V_2}$ in TiO_2•**1** is shifted to more negative potentials than the same reduction in the corresponding axle component TiO_2•**2**. An interesting finding is that the second reduction of $\mathbf{V_2}$ is, within experimental error, at the same potential in TiO_2•**1** and in TiO_2•**2**. On this basis, it is concluded that **C** is not localized at the radical cation of $\mathbf{V_2}$.

This finding suggests that the affinity of **C** for the singly reduced form of $\mathbf{V_2}$ is not sufficient to localize the crown ether

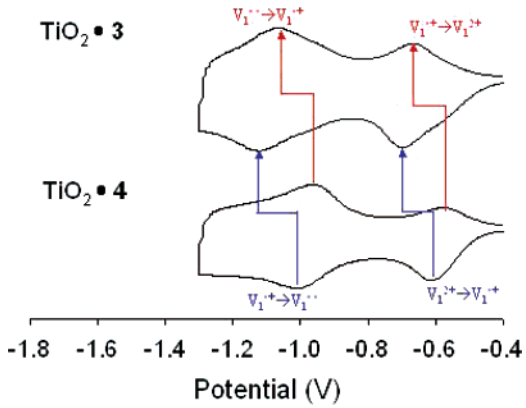

Figure 4. Cyclic voltammograms of nanostructured TiO_2 film (geometric area of 0.8 cm^2, surface roughness of 1000) modified by adsorption of **3** (5×10^{16} molecules) and **4** (5×10^{16} molecules) recorded in acetonitrile containing added TBAP (0.1 mol dm^{-3}) at 25 °C.

at this viologen. Accordingly, **C** may be in motion along the entire length of the axle.

Further insight is provided by considering the difference in the reoxidation potentials of the viologens in TiO_2•**1** and TiO_2•**2**. It is found that the first and second reoxidation potentials of $\mathbf{V_2}$ are shifted to more positive potentials by 44 mV and 4 mV, respectively, due to the presence of **C** in TiO_2•**1**. It is also found that the first and second reoxidation potentials of $\mathbf{V_1}$ are shifted to more positive values by 28 mV and more negative values by 47 mV, respectively.

On this basis, it has been concluded that **C** is not localized at $\mathbf{V_2}$ when this viologen is in either doubly or singly reduced state; otherwise it would be expected that the first and second reoxidation potentials would be shifted to more negative values. This is consistent with the findings above that **C** is not localized at either singly or doubly reduced $\mathbf{V_2}$. What was not expected is the magnitude of the observed shifts in the first and second reoxidation potentials to more positive values. To account for these findings, we propose that there is a conformational change associated with the hetero[2]rotaxane TiO_2•**1** when both viologens are in their doubly reduced state and the crown is free to move along the axle. This conformational change is currently the subject of a detailed study whose findings will be reported in due course.[22]

On this basis, it has also been concluded that **C** is not localized on $\mathbf{V_1}$ when it is in its doubly reduced state but is when it is in its singly reduced state. This accounts for the fact that the first reoxidation potential is shifted to more positive potentials, while the second reoxidation potential is shifted to more negative values. This conclusion is also consistent with that arrived at based on an analysis of the corresponding reduction potentials.

Shown in Figure 4 are the CVs of the tripodal hetero[2]rotaxane TiO_2•**3** and the corresponding axle component adsorbed at the surface of a TiO_2 nanoparticle TiO_2•**4**. It is found that the first and second reduction potentials of $\mathbf{V_1}$ are shifted to more negative values by 85 mV and 100 mV, respectively, in the presence of **C**. It is also found that the first and second reoxidation potentials of $\mathbf{V_1}$ are shifted to more negative values by 102 mV and 87 mV in the presence of added **C**. On this basis, it is concluded that transfer of an electron from the TiO_2 nanoparticle to $\mathbf{V_1}$ to form the corresponding radical cation does not result in **C** being completely dissociated from $\mathbf{V_1}$. These findings are as expected and consistent with those reported above and elsewhere for a closely related system.[13]

Scheme 4. Electrodynamics of Hetero[2]rotaxane

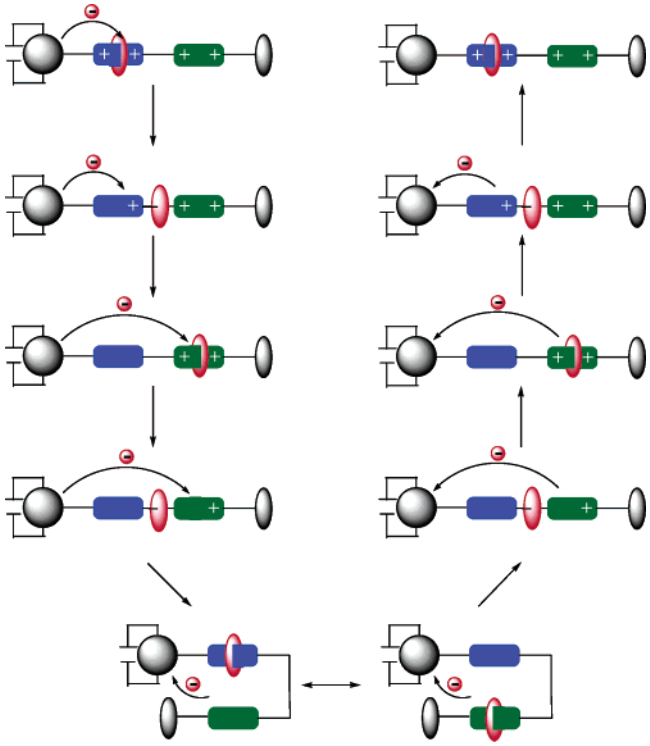

Conclusions

It is concluded that it is possible to electronically address and switch the hetero[2]rotaxane shown in Scheme 1. Specifically, by applying a suitable potential, it is possible to transfer between one and four electrons from the conduction band of the TiO_2 nanoparticle to $\mathbf{V_1}$ adjacent to **L** and $\mathbf{V_2}$ adjacent to **S** of the [2]rotaxane component. As a result, **C** is localized at either $\mathbf{V_1}$ or the $\mathbf{V_2}$.

More specifically, and as shown in Scheme 4, **C** is initially localized on $\mathbf{V_1}$ adjacent to **L**. Following transfer of a single electron to $\mathbf{V_1}$, to form the corresponding radical cation, **C** is no longer localized on $\mathbf{V_1}$ and interacts with both $\mathbf{V_1}$ and $\mathbf{V_2}$ adjacent to **S**. Transfer of a second electron to $\mathbf{V_1}$, to form the corresponding diradical, leads to **C** being localized on $\mathbf{V_2}$.

Following transfer of a single electron to $\mathbf{V_2}$, to form the corresponding radical cation, **C** is no longer localized on $\mathbf{V_2}$ and does not interact strongly with either $\mathbf{V_1}$ or $\mathbf{V_2}$. Transfer of a second electron to $\mathbf{V_2}$, to form the corresponding diradical, is accompanied by a conformational change. This change in conformation is possibly a folding of the fully reduced [2]rotaxane and a stacking of the diradicals of $\mathbf{V_1}$ and $\mathbf{V_2}$ and **C**.

As a consequence of this conformational change, a significantly more positive potential than might have otherwise have been expected, is required to remove the first electron from the fully reduced [2]rotaxane. The subsequent removal of three electrons leads to the localization of **C**, first on $\mathbf{V_2}$ and subsequently in $\mathbf{V_1}$ as shown in Scheme 4.

These findings point the way to the preparation and characterization of a related family of hetero[2]rotaxanes and related

(22) Lestini, E.; Nikitin, K.; Fitzmaurice, D. Manuscript in preparation.

nanoscale components that can be both electronically and optically addressed and switched. These nanoscale components offer potentially significant advantages over purely condensed phase or molecular components.

Experimental Section

Synthesis of Molecular Components. Synthesis of the ester analogues and immediate precursors of the molecular components **1** to **4** shown in Scheme 2 has been described in detail elsewhere.[15] The molecular components **1** to **4** were obtained from their ester precursors as follows: bromotrimethylsilane (0.05 mL) in dioxane (0.25 mL) was added to the ester (3 μmol) in dry 1,4-dioxane (1.00 mL). The resulting mixture was kept at room temperature for 20 h and extracted with concentrated HCl, and the extract was washed with ether (2 × 2 mL) and concentrated under reduced pressure to give the acid as a glassy solid (3 μmol, 100%). The crown ether **5** was synthesized following literature methods.[21] The stabilizer **6** was synthesized as described in detail elsewhere.[13b]

The results of the characterization of these compounds are given below. Melting points were estimated using a Gallenkamp melting point device and were not corrected. NMR spectra were recorded using Varian Inova 300 and 500 spectrometers in the indicated solvent at 30 °C. Proton NMR spectra were recorded at 299.89 and 499.82 MHz, and phosphorus NMR spectra, at 121.39 MHz. Mass spectra were recorded on a Micromass LCT KC 420 mass spectrometer.

Compound 1. 1-{4-[Tris{4-(4-dihydrophosphonophenyl)-pheny}-methyl]phenyl}-1′-(3-[3,3′-dimethyl-1′-(4-[bis{4-*tert*-butylphenyl}-4-ethylphenylmethyl]phenoxyethoxyethoxyphenylmethyl)-4,4′-bipyridyl-1-yl]propyl)-4,4′-bipyridinium 34-crown-10 tetrachloride: ^{1}H NMR (CD_3OD) δ 9.34 (s, 1H), 9.33 (d, 2H, J = 7 Hz), 9.15 (d, 2H, J = 7 Hz), 9.15 (d, 1H, J = 7 Hz), 9.10 (s, 1H), 8.90 (d, 1H, J = 7 Hz), 8.34 (d, 2H, J = 7 Hz), 8.13 (d, 1H, J = 7 Hz), 8.11 (d, 2H, J = 7 Hz), 8.05 (d, 1H, J = 7 Hz), 7.90 (d, 1H, J = 7 Hz), 7.8 (m, 10 H), 7.65 (m, 6H), 7.55 (d, 6H, J = 9 Hz), 7.38 (d, 6H, J = 9 Hz), 7.15 (d, 4H, J = 9 Hz), 7.0 (m, 14H), 6.69 (d, 2 H, J = 9 Hz), 6.20 (s, 8 H), 5.75 (s, 2H), 5.1 (m, 4 Hz), 4.1 (m, 4 H), 3.8 (m, 4H), 3.6 (m, 24H), 3.5 (m, 8H), 3.1 (m, 2H), 2.50 (q, 2H, J = 7 Hz), 2.32 (s, 6H), 1.20 (s, 18 H), 1.12 (t, 3H, J = 7 Hz); ^{31}P NMR δ 18.4 (s); MS (*m*/*z*) 2468 (MCl_3^{2+}).

Compound 2. 1-{4-[Tris{4-(4-dihydrophosphonophenyl)pheny}-methyl]phenyl}-1′-(3-[3,3′-dimethyl-1′-(4-[bis{4-*tert*-butylphenyl}-4-ethylphenylmethyl]phenoxyethoxyethoxyphenylmethyl)-4,4′-bipyridyl-1-yl]propyl)-4,4′-bipyridinium tetrachloride: ^{1}H NMR (CD_3OD) δ 9.53 (d, 2H, J = 7 Hz), 9.38 (d, 2H, J = 7 Hz), 9.36 (s, 1H), 9.20 (d, 1H, J = 7 Hz), 9.10 (s, 1H), 8.89 (d, 1H, J = 7 Hz), 8.79 (d, 2H, J = 7 Hz), 8.65 (d, 2H, 7 Hz), 8.07 (d, 1H, J = 7 Hz), 7.91(d, 1H, J = 7 Hz), 7.8 (m, 10 H), 7.65 (m, 6H), 7.58 (m, 6H, J = 9 Hz), 7.38 (d, 6H, J = 9 Hz), 7.18 (d, 4H, J = 9 Hz), 7.0 (m, 14H), 6.72 (d, 2 H, J = 9 Hz), 5.77 (s, 2H), 5.1 (t, 2H, J = 6 Hz), 5.00 (t, 2H, J = 6 Hz), 4.1 (m, 4 H), 3.8 (m, 4H), 2.95 (m, 2H), 2. 55 (q, 2H, J = 7 Hz), 2.29 (s, 6H), 1.22 (s, 18 H), 1.20 (t, 3H, J = 7 Hz); ^{31}P NMR δ 18.4 (s); MS (*m*/*z*) 1929 (MCl_3^+ − H).

Compound 3. 1-{4-[Tris{4-(4-dihydrophosphonophenyl)pheny}-methyl]phenyl}-1′-4-(4-[tris{4-*tert*-butylphenyl}methyl]phenoxymethyl)-phenylmethyl)-4,4′-bipyridinium bis-paraphenylene-34-crown-10 dichloride: ^{1}H NMR (CD_3OD) δ 9.36 (d, 2H, J = 7 Hz), 8.86 (d, 2H, J = 7 Hz), 8.36 (d, 2H, J = 7 Hz), 8.11 (d, 2H, J = 7 Hz), 7.8 (m, 8 H), 7.65 (m, 8H), 7.58 (m, 6H), 7.45 (m, 6H), 7.18 (d, 6H, J = 9 Hz), 7.0 (m, 12 H), 6.70 (d, 2 H, J = 9 Hz), 6.10 (s, 8H), 5.86 (s, 2H), 4.1 (m, 4 H), 3.8 (m, 4H), 3.5 (m, 16H), 3.4 (m, 8H), 1.22 (s, 27 H); ^{31}P NMR δ 18.4 (s); MS (*m*/*z*) 1622 (M^{2+} − 2H).

Compound 4. 1-{4-[Tris{4-(4-dihydrophosphonophenyl)pheny}-methyl]phenyl}-1′-4-(4-[tris{4-*tert*-butylphenyl}methyl]phenoxymethyl)-phenylmethyl)-4,4′-bipyridinium dichloride: ^{1}H NMR (CD_3OD) δ 9.36 (d, 2H, J = 7 Hz), 9.20 (d, 2H, J = 7 Hz), 8.76 (d, 2H, J = 7 Hz), 8.65 (d, 2H, J = 7 Hz), 7.8 (m, 8 H), 7.65 (m, 6H), 7.57 (m, 6H), 7.4 (m, 8H), 7.18 (d, 6H, J = 9 Hz), 7.0 (m, 12 H), 6.72 (d, 2 H, J = 9 Hz), 5.80 (s, 2H), 4.1 (m, 4 H), 3.8 (m, 4H), 1.22 (s, 27 H); ^{31}P NMR δ 18.4 (s); MS (*m*/*z*) 1080 (M^+ − 2H).

Compound 5. Bis-paraphenylene-34-crown-10 was prepared according to a known procedure as a white solid:[21] mp 90 °C (lit.[21] mp 88 °C);^{1}H NMR (CD_3CN) δ 6.63 (s, 8H), 3.75 (m, 8H), 3.6 (m, 8H), 3.5 (m, 16 H).

Compound 6. 1-Phosphonoethylperdeuteriopyridinium bromide was obtained as a white solid (yield 80%):[13] mp 154 °C; ^{1}H NMR (CD_3OD) δ 9.09 (trace), 8.67 (trace), 8.16 (trace), 4.92 (q, 2H, J = 7 Hz), 4.8 (s, 2H), 2.6 (m, 2H); ^{31}P NMR (CD_3OD) δ 22.1 (s). Anal. Calcd for $C_7H_6D_5BrNO_3P$: C, 30.79; H, 5.90; N, 5.13; Br, 29.26. Found: C, 31.15; H, 5.96; N, 5.17; Br, 29.08.

Preparation of Titanium Dioxide Nanoparticle Aqueous Dispersions. An aqueous dispersion of titanium dioxide nanoparticles was prepared by the hydrolysis of titanium tetraisopropoxide at pH 2 as described in detail elsewhere.[18] Refluxing the initially formed dispersion at 80 °C for 8 h evaporates the principal side product 2-propanol and promotes crystallization of the nanoparticles. The average diameter of the TiO_2 nanoparticles was determined by TEM to be 6 nm. X-ray diffraction confirmed their crystal structure to be anatase. The final concentration of TiO_2 nanoparticles was determined by dry weight measurements to be 3.2% w/w.

Preparation of Modified Nanoparticles. An aqueous dispersion of TiO_2 nanoparticles (1 mL) was transferred to a glass centrifuge tube and was diluted with methanol (to 10 mL) yielding a dispersion of a known particle concentration (1.2×10^{-5} mol dm^{-3}). A known amount (1.5×10^{-6} mol) of the tripodal [2]rotaxane **1** or **3** (or the corresponding tripodal axle **2** or **4**) was dissolved in $CHCl_3$/MeOH (1:1 by vol) and added dropwise to the above dispersion of TiO_2 nanoparticles while stirring vigorously. Stirring was continued for 10 min. A known weight (2.4×10^{-5} mol) of the stabilizer **6** was dissolved in MeOH (1 mL) and added dropwise to the above stirring dispersion. Stirring was continued for 1 h. To induce counterion exchange and precipitation of the modified nanoparticles, NH_4PF_6 was added in large excess (1.0×10^{-3} mol). The precipitate was centrifuged and washed with dry MeOH (5 mL). The last step was repeated 3 times to remove all the residual water. Finally the precipitate was sonicated in acetonitrile (3 mL) for 1 h to redisperse the nanoparticles. The resulting dispersion was optically transparent.

Preparation of Transparent Nanostructured TiO_2 Films. Transparent nanostructured TiO_2 films were deposited on F-doped tin oxide glass substrates (10 Ω units, 0.5 μm thick, supplied by Glastron). Specifically, an aqueous colloidal dispersion of TiO_2 was prepared as described above and autoclaved at 200 °C for 12 h to yield a dispersion of 12 nm diameter nanocrystals.[18] Concentration of this dispersion (160 g L^{-1}) and addition of Carbowax 20000 (40 wt % equiv of TiO_2) yields a viscous paste. This paste was spread using a glass rod on the conducting glass substrate masked by scotch tape. Following drying in air for 1 h, the film was fired, also in air at 450 °C for 12 h. The resulting transparent nanostructured electrodes are 4 μm thick.

Modification of Transparent Nanostructured TiO_2 Films. A transparent nanostructured TiO_2 film was immersed in a dry acetonitrilic solution (1×10^{-3} mol dm^{-3}) of the tripodal [2] rotaxane **1** or **3** (or the corresponding axle component **2** or **4**, respectively) for 1 h at room temperature. The modified film was removed from the above solution and washed thoroughly with dry ethanol. The modified films were dried using a hot air gun (at approximately 80 °C) before being stored in a desiccator until required for use. The active area of the film is 0.8 cm^2 (geometric area) × 1000 (surface roughness), which is 800 cm^2. The density of sites at which a phosponate linker may be adsorbed is 2×10^{14} cm^{-2}.[19] On this basis, it is estimated that there are approximately 5×10^{16} tripodal [2]rotaxanes (or the corresponding axle components) adsorbed at the surface of the TiO_2 film.

Paramagnetic Suppression Nuclear Magnetic Resonance Spectroscopy. To measure a PASSY (paramagnetic suppression) NMR spectrum of a solution of a given molecular component in acetonitrile,[23] a known volume of the sample (1 mL), was first deoxygenated by bubbling with nitrogen. Zinc metal powder (200 mesh, 10 mg) was then added.[20,21] The sample continued to be degassed by bubbling with nitrogen. After 30 min, the dispersion became deeply colored indicating formation of a radical cation of the viologen, and the proton NMR spectrum was measured.

To measure a PASSY (paramagnetic suppression) NMR spectrum of a dispersion of modified nanoparticles in acetonitrile,[23] a known volume of the sample (1 mL) was first deoxygenated by bubbling with nitrogen. Chromium trichloride (0.2 mg) was then added and solubilized by sonication for 30 min, followed by Zn metal powder (200 mesh, 10 mg).[20,21] The sample continued to be degassed by bubbling with nitrogen. After 30 min, the dispersion became deeply colored indicating formation of a radical cation of the viologen, and the proton NMR spectrum was measured.

Optical Absorption Spectroscopy. All optical absorption spectra were recorded at 25 °C using a Hewlett-Packard 8452A diode array spectrometer controlled by a LabView program running on a Macintosh Power PC. All samples were contained in a 1.0 cm quartz cuvette.

Cyclic Voltammetry. All cyclic voltammograms (CVs) were recorded in solution under the following conditions: The working electrode (WE) was an isolated platinum wire. The counter electrode (CE) was isolated platinum gauze. The reference electrode (RE) was a nonaqueous Ag/Ag^+ electrode filled with 10 mM $AgNO_3$ in the electrolyte solution. The electrolyte solution was tetrabutylammonium perchlorate (TBAP, 0.1 mol dm^{-3}) in dry acetonitrile. All solutions were bubbled with argon gas for 20 min prior to measurement. All cyclic voltammograms were recorded on a Solartron SI 1287 potentiostat controlled by a LabView program running on a Machintosh Power PC at a scan rate of 20 mV s^{-1} unless otherwise stated.

All CVs were recorded for nanostructured TiO_2 films under the following conditions: The WE was a nanostructured TiO_2 film. The CE was isolated platinum gauze. The RE was a nonaqueous Ag/Ag^+ electrode filled with 10 mM $AgNO_3$ in the electrolyte solution. The electrolyte solution was TBAP (0.1 mol dm^{-3}) in dry acetonitrile. All solutions were bubbled with argon gas for 20 min prior to measurement. As above all CVs were recorded on a Solartron SI 1287 potentiostat controlled by a LabView program running on a Machintosh Power PC at a scan rate of 20 mV s^{-1} unless otherwise stated.

Supporting Information Available: Syntheses of the tripodal viologen and related molecular components employed in this study. This material is available free of charge via the Internet at http://pubs.acs.org.

JA037592G

(23) Carrington, A.; McLachlan, A. D. *Introduction to Magnetic Resonance*; Harper and Row: New York, 1967.